Available online at www.sciencedirect.com
ScienceDirect
Comput. Methods Appl. Mech. Engrg. 278 (2014) 347–360
Computer methods in applied mechanics and engineering
www.elsevier.com/locate/cma

A finite difference scheme for multidimensional convection–diffusion–reaction equations

A. Kaya*

Department of Mathematics, Izmir Institute of Technology, 35430 Izmir, Turkey

Received 29 March 2014; received in revised form 21 May 2014; accepted 2 June 2014
Available online 11 June 2014

Abstract

In this paper a finite difference scheme is proposed for multidimensional convection–diffusion–reaction equations, particularly designed to treat the most interesting case of small diffusion. It is based closely on the work Şendur and Neslitürk (2011). Application of the method to multidimensional convection–diffusion–reaction equation is based on a simple splitting of the convection–diffusion–reaction equation and then joining their approximations obtained with Şendur and Neslitürk (2011). The method adapts very well to all regimes with continuous transitions from one regime to another. Numerical tests show good performance of the method and superiority with respect to well known stabilized finite element methods.

Keywords: Finite difference method; Finite element method; Advection–diffusion–reaction

1. Introduction

Exact solution of the convection–diffusion–reaction equation may contain sharp layers where gradient of the solution changes abruptly when the problem is convection-dominated or reaction-dominated. In such cases, classical numerical approaches such as standard Galerkin and central differencing do not work and exhibit spurious oscillations that pollute whole domain. Many methods have been proposed so far to cure this situation, especially in finite element approach.

In the context of variational formulations, Streamline-Upwind Petrov Galerkin (SUPG) [1] is one of the first method to cure this situation. Another approach is Residual-Free-Bubble (RFB) method based on enriching the finite element space [2–5]. It is first studied in [3] to find a suitable value of stabilizing parameter for SUPG method. The main problem with this method is that it requires the solution of a local PDE which is as difficult as solving the original problem. Cheap approximate solutions to this local problem were designed by several researchers [6–15]. Although there exist very effective algorithms in one space dimension such as [6,15], in higher dimensions, it is very difficult to design methods which are robust in all regimes and the techniques have been proposed so far to approximate the local PDE are not efficient as in one space dimension (see [14,15]).

* Tel.: +90 02327507773.
E-mail addresses: ademkaya@iyte.edu.tr, baffiros@gmail.com.

http://dx.doi.org/10.1016/j.cma.2014.06.002
0045-7825/

Pseudo Residual-Free Bubble (P-RFB) [15] method aims to get sub-grid nodes to approximate bubble functions cheaply using piecewise linear functions by a minimization process with respect to L_1 norm. It adapts very well to all regimes with continuous transitions from one regime to another regime. Although it is applicable in two and three space dimensions, it is not easy to find optimal positions of sub-grid nodes to approximate bubble functions (see [14]). Piecewise linear approximation to bubble functions in [15] is the main motivation to start this work.

It is well known that standard Galerkin finite element method with piecewise linear basis functions corresponds to central differencing on uniform meshes. Since the pseudo bubble functions used in [15] are piecewise linear, it is possible to find finite difference correspondence of the integrals containing bubble functions and thus, finite difference correspondence of [15]. Hauke and his coworkers did similar works to examine stability of Galerkin, SUPG and SGS/GSGS methods for time dependent convection–diffusion–reaction equations in [16–18].

In this study we aim to find finite difference correspondence of the method [15]. To apply the method in multidimensions a simple splitting is done for convection–diffusion–reaction equation and then their approximations obtained with the finite difference correspondence of [15] are joined together.

The paper is organized as follows: In the next section, a brief review of P-RFB [15] method and its finite difference correspondence are given. In Section 3, application of the method in two space dimensions is given. We give numerical experiments to illustrate the performance of the proposed method in Section 4. Finally, concluding remarks.

2. Pseudo Residual-Free Bubble (P-RFB) method [15] and its finite difference correspondence

We start with considering the following one dimensional convection–diffusion–reaction equation:

$$\begin{cases} \mathcal{L}u = -\epsilon u'' + \beta u' + \sigma u = f(x) \quad \text{on } I, \\ u(a) = u(b) = 0, \end{cases} \tag{1}$$

where $I = (a, b)$, $\epsilon > 0$, $\beta \geq 0$ and $\sigma \geq 0$ for simplicity. P-RFB method [15] was designed for Eq. (1). It aims to approximate the basis bubble functions with piecewise linear functions by adding sub-grid nodes in each element (see Fig. 1). Let z_1 and z_2 be two sub-grids in a typical element $K = (x_{k-1}, x_k)$ such that $x_{k-1} < z_1 < z_2 < x_k$ on which the basis bubble functions are approximated. Explicit expressions of the heights α_1 and α_2 of the pseudo-bubbles are defined as follows:

$$\alpha_1 = \frac{3\beta + (\xi - 2h)\sigma}{2h(\frac{3\epsilon}{\xi(h-\xi)} + \sigma)}, \qquad \alpha_2 = -\frac{3\beta + (2h - \eta)\sigma}{2h(\frac{3\epsilon}{\eta(h-\eta)} + \sigma)} \tag{2}$$

where $\xi = z_1 - x_{k-1}$, $\eta = x_k - z_2$. We note that optimal choice of ξ in convection dominated regime is $h - \eta$ (see Fig. 2). Then locations of the sub-grid nodes z_i $(i = 1, 2)$ are defined as follows:

$$\begin{aligned} x_2 - z_2 &= \min\left\{\frac{h}{3}, \frac{-3\beta + \sqrt{9\beta^2 + 24\epsilon\sigma}}{2\sigma}\right\}, \\ z_1 - x_1 &= \min\left\{h - \eta, \frac{3\beta + \sqrt{9\beta^2 + 24\epsilon\sigma}}{2\sigma}\right\}. \end{aligned} \tag{3}$$

After finding the locations of sub-grids, P-RFB reads on extended space $V_h = V_L \bigoplus V_B$: Find u_h in V_h such that

$$a(u_L, v_h) + a(u_B, v_h) = (f, v_h), \quad \forall v_h \in V_h \tag{4}$$

where V_L is the space of continuous piecewise linear polynomials and $V_B = \bigoplus_K B_K$ is the space of continuous piecewise linear bubble functions such that $B_K = H_0^1(K)$ and bilinear form is defined as follows:

$$a(u, v) = \epsilon \int_I u'v'dx + \int_I (\beta u)'v dx + \int_I uv dx. \tag{5}$$

In order to derive finite difference correspondence of [15] we calculate the integrals coming from the variational formulation. We omit calculations of the integrals and directly give results. Let u_j represent the numerical approximation

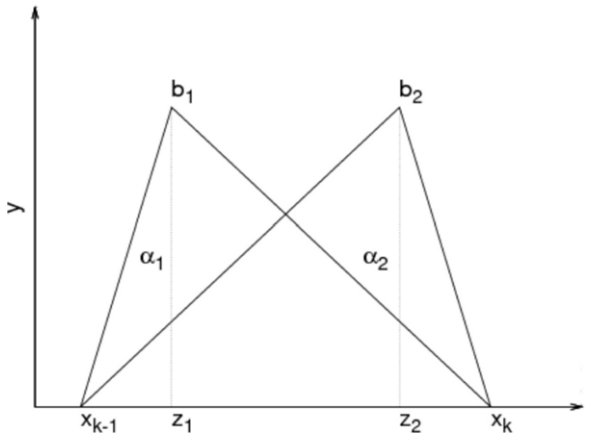

Fig. 1. Pseudo basis bubble functions.

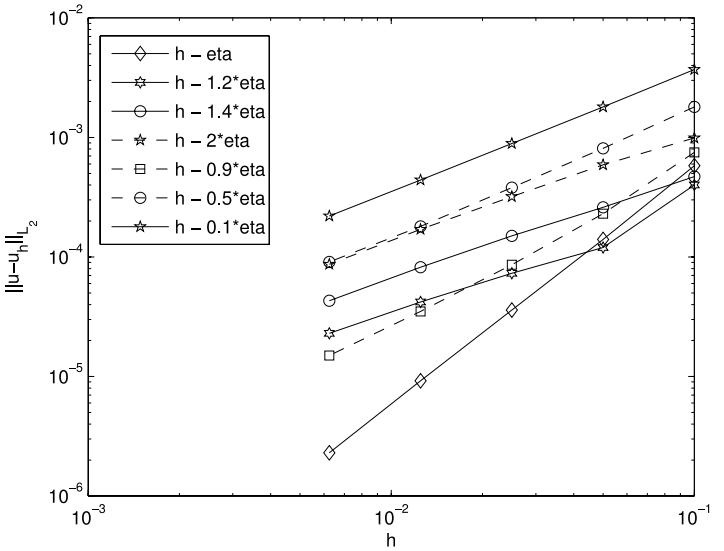

Fig. 2. Optimal ξ in convection — dominated regime.

at node x_j. Combining all the results and dividing both sides by h we get finite difference correspondence of [15] on uniform mesh as follows:

$$
\begin{aligned}
&-\epsilon\frac{u_{j+1}-2u_j+u_{j-1}}{h^2}+\beta\frac{u_{j+1}-u_{j-1}}{2h}+\sigma\frac{u_{j+1}+4u_j+u_{j-1}}{6}\\
&\quad+\beta\frac{\alpha_2}{2}\left(\frac{u_{j+1}-u_j}{h}\right)+\beta\frac{\alpha_1}{2}\left(\frac{u_j-u_{j-1}}{h}\right)\\
&\quad+\sigma\frac{\alpha_2(h+\eta)u_{j+1}+(\alpha_2(2h-\eta)+\alpha_1(2h-\xi))\,u_j+\alpha_1(h+\xi)u_{j-1}}{6h}\\
&=\frac{f_{j-1}+4f_j+f_{j+1}}{6}+\frac{\alpha_2(h+\eta)f_{j+1}+(\alpha_2(2h-\eta)+\alpha_1(2h-\xi))\,f_j+\alpha_1(h+\xi)f_{i-1}}{6h}.
\end{aligned}
\tag{6}
$$

On non-uniform meshes the right hand side requires a special attention for variable case when the problem is reaction-dominated. So, we give finite difference correspondence without source function on non-uniform meshes as follows:

$$
-\epsilon\frac{u_{j+1}}{h_2}+\epsilon\frac{u_j}{h_2}+\epsilon\frac{u_j}{h_1}-\epsilon\frac{u_{j-1}}{h_1}+\beta\frac{u_{j+1}-u_{j-1}}{2}+\sigma\frac{h_2u_{j+1}+2h_2u_j+2h_1u_j+h_1u_{j-1}}{6}
$$

$$+\beta\left(\alpha_{22}\frac{u_{j+1}}{2}+\alpha_{21}\frac{u_j}{2}-\alpha_{12}\frac{u_j}{2}-\alpha_{11}\frac{u_{j-1}}{2}\right)$$
$$+\sigma\frac{\alpha_{22}(h_2+\eta_2)u_{j+1}+(\alpha_{12}(2h_1-\eta_1)+\alpha_{21}(2h_2-\xi_2))\,u_j+\alpha_{11}(h_1+\xi_1)u_{j-1}}{6}=0 \tag{7}$$

where $h_2=x_{j+1}-x_j$, $h_1=x_j-x_{j-1}$. While α_{22}, α_{21}, η_2 and ξ_2 are calculated in the interval (x_j, x_{j+1}), α_{12}, α_{11}, η_1 and ξ_1 are calculated in the interval (x_{j-1}, x_j).

3. Application of the method to 2-dimensional convection–diffusion–reaction equations

Now, we consider the following constant coefficient linear elliptic convection–diffusion–reaction problem in a polygonal domain Ω:

$$\begin{cases}-\epsilon\left(\dfrac{\partial^2 u}{\partial x^2}+\dfrac{\partial^2 u}{\partial y^2}\right)+b.\left(\dfrac{\partial u}{\partial x},\dfrac{\partial u}{\partial y}\right)+\sigma u=f(x,y) \quad \text{on } \Omega,\\ u(x,y)=0 \quad \text{on } \partial\Omega,\end{cases} \tag{8}$$

under the assumptions that $\epsilon>0$, $b=(b_1,b_2)\neq 0$. We can rewrite Eq. (8) as follows:

$$\begin{cases}-\epsilon\left(\dfrac{\partial^2 u}{\partial x^2}\right)+b_1\left(\dfrac{\partial u}{\partial x}\right)+\sigma\dfrac{|b_1|}{|b_1|+|b_2|}u-\epsilon\left(\dfrac{\partial^2 u}{\partial y^2}\right)+b_2\left(\dfrac{\partial u}{\partial y}\right)+\sigma\dfrac{|b_2|}{|b_1|+|b_2|}u\\ \quad=\dfrac{|b_1|}{|b_1|+|b_2|}f(x,y)+\dfrac{|b_2|}{|b_1|+|b_2|}f(x,y) \quad \text{on } \Omega,\\ u(x,y)=g \quad \text{on } \partial\Omega.\end{cases} \tag{9}$$

Next, we consider Eq. (9) as a sum of the following one space dimensional convection–diffusion–reaction equations;

$$\begin{cases}-\epsilon\left(\dfrac{d^2u}{dx^2}\right)+b_1\left(\dfrac{du}{dx}\right)+\sigma\dfrac{|b_1|}{|b_1|+|b_2|}u=\dfrac{|b_1|}{|b_1|+|b_2|}f,\\ -\epsilon\left(\dfrac{d^2u}{dy^2}\right)+b_2\left(\dfrac{du}{dy}\right)+\sigma\dfrac{|b_2|}{|b_1|+|b_2|}u=\dfrac{|b_2|}{|b_1|+|b_2|}f.\end{cases} \tag{10}$$

Summing up their approximations obtained with finite difference scheme (6) we get the following finite difference approximation for Eq. (8);

$$\begin{aligned}
&-\epsilon\frac{u_{i+1,j}-2u_{i,j}+u_{i-1,j}}{h^2}+b_1\frac{u_{i+1,j}-u_{i-1,j}}{2h}+b_1\frac{\alpha_{x2}}{2}\left(\frac{u_{i+1,j}-u_{i,j}}{h}\right)+b_1\frac{\alpha_{x1}}{2}\left(\frac{u_{i,j}-u_{i-1,j}}{h}\right)\\
&\quad+\frac{|b_1|}{|b_1|+|b_2|}\left(\sigma\frac{u_{i+1,j}+4u_{i,j}+u_{i-1,j}}{6}\right.\\
&\quad\left.+\ \sigma\frac{\alpha_{x2}(h+\eta_x)u_{i+1,j}+(\alpha_{x2}(2h-\eta_x)+\alpha_{x1}(2h-\xi_x))\,u_{i,j}+\alpha_{x1}(h+\xi_x)u_{i-1,j}}{6h}\right)\\
&\quad-\epsilon\frac{u_{i,j+1}-2u_{i,j}+u_{i,j-1}}{k^2}+b_2\frac{u_{i,j+1}-u_{i,j-1}}{2k}+b_2\frac{\alpha_{y2}}{2}\left(\frac{u_{i,j+1}-u_{i,j}}{k}\right)+b_2\frac{\alpha_{y1}}{2}\left(\frac{u_{i,j}-u_{i,j-1}}{k}\right)\\
&\quad+\frac{|b_2|}{|b_1|+|b_2|}\left(\sigma\frac{u_{i,j+1}+4u_{i,j}+u_{i,j-1}}{6}\right.\\
&\quad\left.+\sigma\frac{\alpha_{y2}(k+\eta_y)u_{i,j+1}+\left(\alpha_{y2}(2k-\eta_y)+\alpha_{y1}(2k-\xi_y)\right)u_{i,j}+\alpha_{y1}(k+\xi_y)u_{i,j-1}}{6k}\right)\\
&=\frac{|b_1|}{|b_1|+|b_2|}\left(\frac{f_{i-1,j}+4f_{i,j}+f_{i+1,j}}{6}\right.\\
&\quad\left.+\ \frac{\alpha_{x2}(h+\eta_x)f_{i+1,j}+(\alpha_{x2}(2h-\eta_x)+\alpha_{x1}(2h-\xi_x))\,f_{i,j}+\alpha_{x1}(h+\xi_x)f_{i-1,j}}{6h}\right)
\end{aligned}$$

$$+\frac{|b_2|}{|b_1|+|b_2|}\left(\frac{f_{i,j-1}+4f_{i,j}+f_{i,j+1}}{6}\right.$$
$$\left.+\frac{\alpha_{y2}(k+\eta_y)f_{i,j+1}+\left(\alpha_{y2}(2k-\eta_y)+\alpha_{y1}(2k-\xi_y)\right)f_{i,j}+\alpha_{y1}(k+\xi_y)f_{i,j-1}}{6k}\right). \tag{11}$$

The sub-indices x and y in α_1, α_2, ξ and η represent discretizations in which they are obtained. Since the source function requires a special attention for variable case on non-uniform meshes, we give finite difference approximation of convection–diffusion–reaction equation (8) without source function as follows:

$$\begin{aligned}
&-\epsilon\frac{u_{i+1,j}}{h_2}+\epsilon\frac{u_{i,j}}{h_2}+\epsilon\frac{u_{i,j}}{h_1}-\epsilon\frac{u_{i-1,j}}{h_1}+b_1\frac{u_{i+1,j}-u_{i-1,j}}{2}\\
&+b_1\left(\alpha_{x22}\frac{u_{i+1,j}}{2}+\alpha_{x21}\frac{u_{i,j}}{2}-\alpha_{x12}\frac{u_{i,j}}{2}-\alpha_{x11}\frac{u_{i-1,j}}{2}\right)\\
&+\frac{|b_1|}{|b_1|+|b_2|}\sigma\ \frac{h_2u_{i+1,j}+2h_2u_{i,j}+2h_1u_{i,j}+h_1u_{i-1,j}}{6}+\frac{|b_1|}{|b_1|+|b_2|}\sigma\\
&\times\frac{\alpha_{x22}(h_2+\eta_{x2})u_{i+1,j}+(\alpha_{x12}(2h_1-\eta_{x1})+\alpha_{x21}(2h_2-\xi_{x2}))\,u_{i,j}+\alpha_{x11}(h_1+\xi_{x1})u_{i-1,j}}{6}\\
&-\epsilon\frac{u_{i,j+1}}{k_2}+\epsilon\frac{u_{i,j}}{k_2}+\epsilon\frac{u_{i,j}}{k_1}-\epsilon\frac{u_{i,j-1}}{k_1}+b_2\frac{u_{i,j+1}-u_{i,j-1}}{2}\\
&+b_2\left(\alpha_{y22}\frac{u_{i,j+1}}{2}+\alpha_{y21}\frac{u_{i,j}}{2}-\alpha_{y12}\frac{u_{i,j}}{2}-\alpha_{y11}\frac{u_{i,j-1}}{2}\right)\\
&+\frac{|b_2|}{|b_1|+|b_2|}\sigma\ \frac{k_2u_{i,j+1}+2k_2u_{i,j}+2k_1u_{i,j}+k_1u_{i,j-1}}{6}+\frac{|b_2|}{|b_1|+|b_2|}\sigma\\
&\times\frac{\alpha_{y22}(k_2+\eta_{y2})u_{i,j+1}+\left(\alpha_{y12}(2k_1-\eta_{y1})+\alpha_{y21}(2k_2-\xi_{y2})\right)u_{i,j}+\alpha_{y11}(k_1+\xi_{y1})u_{i,j-1}}{6}=0
\end{aligned} \tag{12}$$

where $h_2=x_{i+1}-x_i$, $h_1=x_i-x_{i-1}$, $k_2=y_{i+1}-y_i$ and $k_1=y_i-y_{i-1}$ are projected intervals onto the axes. While α_{x22}, α_{x21}, η_{x2} and ξ_{x2} are calculated in the interval (x_i, x_{i+1}), α_{x12}, α_{x11}, η_{x1} and ξ_{x1} are calculated in the interval (x_{i-1}, x_i). Similarly, the values in y-direction are calculated in the projected intervals (y_i, y_{i+1}) and (y_{i-1}, y_i). Finite difference approximation of Eq. (8) without reaction term on non-uniform grid is suggested as given below:

$$\begin{aligned}
&-\epsilon\frac{u_{i+1,j}}{h_2}+\epsilon\frac{u_{i,j}}{h_2}+\epsilon\frac{u_{i,j}}{h_1}-\epsilon\frac{u_{i-1,j}}{h_1}+b_1\frac{u_{i+1,j}-u_{i-1,j}}{2}\\
&+b_1\left(\alpha_{x22}\frac{u_{i+1,j}}{2}+\alpha_{x21}\frac{u_{i,j}}{2}-\alpha_{x12}\frac{u_{i,j}}{2}-\alpha_{x11}\frac{u_{i-1,j}}{2}\right)\\
&-\epsilon\frac{u_{i,j+1}}{k_2}+\epsilon\frac{u_{i,j}}{k_2}+\epsilon\frac{u_{i,j}}{k_1}-\epsilon\frac{u_{i,j-1}}{k_1}+b_2\frac{u_{i,j+1}-u_{i,j-1}}{2}\\
&+b_2\left(\alpha_{y22}\frac{u_{i,j+1}}{2}+\alpha_{y21}\frac{u_{i,j}}{2}-\alpha_{y12}\frac{u_{i,j}}{2}-\alpha_{y11}\frac{u_{i,j-1}}{2}\right)\\
&=\frac{|b_1|}{|b_1|+|b_2|}\sigma\ \frac{h_2f_{i+1,j}+2h_2f_{i,j}+2h_1f_{i,j}+h_1f_{i-1,j}}{6}\\
&+\frac{|b_2|}{|b_1|+|b_2|}\sigma\ \frac{k_2f_{i,j+1}+2k_2f_{i,j}+2k_1u_{i,j}+k_1f_{i,j-1}}{6}.
\end{aligned} \tag{13}$$

We are doing everything on stencil level. If discretization of a domain can be done with triangular or rectangular elements then we can apply this strategy on the same discretization.

The reason for choices of the coefficients of reaction term and source function in Eq. (10) is to minimize residual coming from the discretization of the problem. Suppose that b_1 and the source function f are zero. Since we are considering small diffusion, we can neglect the error coming from discretization of the diffusion term. If we choose coefficient of reaction term of the first equation in (10) zero then residual becomes approximately zero which comes from just discretization of the diffusion term for the first equation.

We remark that all procedure is applicable in three space dimensions, by splitting convection–diffusion–reaction equation into three equations.

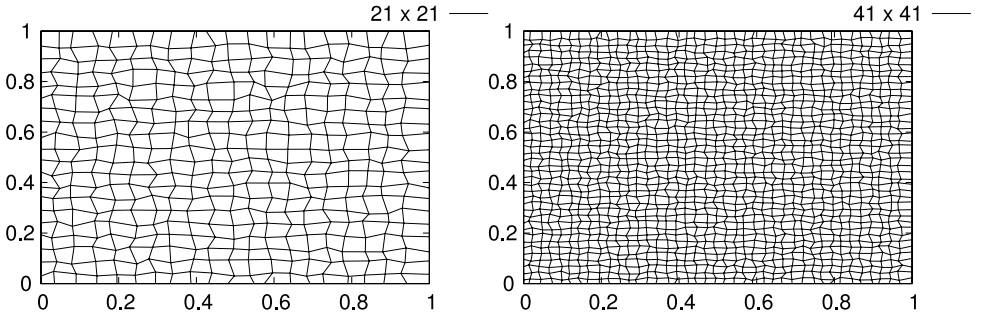

Fig. 3. Examples of unstructured grids.

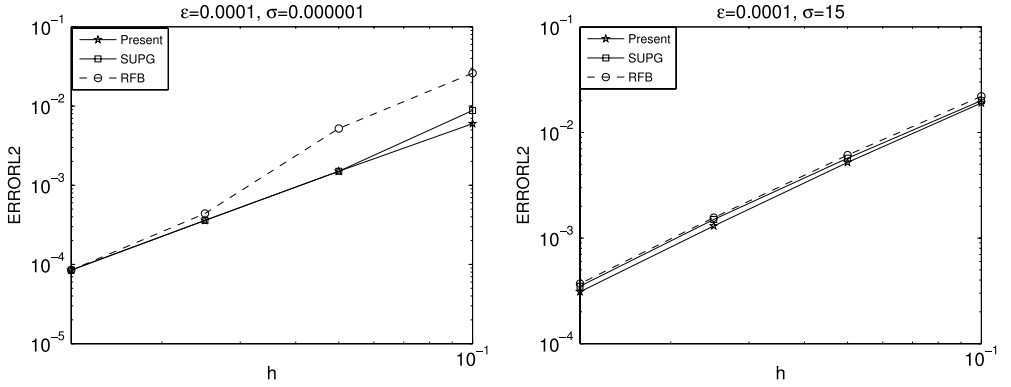

Fig. 4. Test 1, convergence rates of SUPG, RFB and Present methods.

4. Numerical tests

In this section, we report some numerical experiments to illustrate the performance of the present method and compare it with well-known stabilized finite element methods. We report also errors in L_2 norm and non-dimensional parameters; the element Peclet number and the element Damköhler number. The method is tested on both structured and unstructured grids. Unstructured grids are obtained with perturbing internal nodes of structured grids. Fig. 3 shows two examples of unstructured grid obtained with this procedure. RFB solutions are obtained with two level finite element method.

4.1. Test 1

To test the convergence of the method we consider the problem on unit square which is possible to solve analytically with the following boundary conditions:

$$u = \begin{cases} 0, & \text{if } y = 0,\ 0 \le x \le 1, \\ 0, & \text{if } x = 1,\ 0 \le y \le 1, \\ 0, & \text{if } y = 1,\ 0 \le x \le 1, \\ \sin(\pi y), & \text{if } x = 0,\ 0 \le y \le 1. \end{cases}$$

We set $b = (1, 0)$ and $f(x, y) = 0$. The exact solution is

$$u(x, y) = \frac{e^{x/2\epsilon}\ \sinh(-m(1-x))\ \sin(\pi y)}{\sinh(-m)} \quad \text{where } m = \sqrt{1 + 4\epsilon(\epsilon\pi^2 + \sigma)}/2\epsilon.$$

Taking $h = 0.1, 0.05, 0.025, 0.0125$ uniform grid sizes in x and y directions we report errors in L_2 norm. Convergence rates of SUPG, RFB and present methods are presented in Fig. 4 for two different values of reaction coefficient

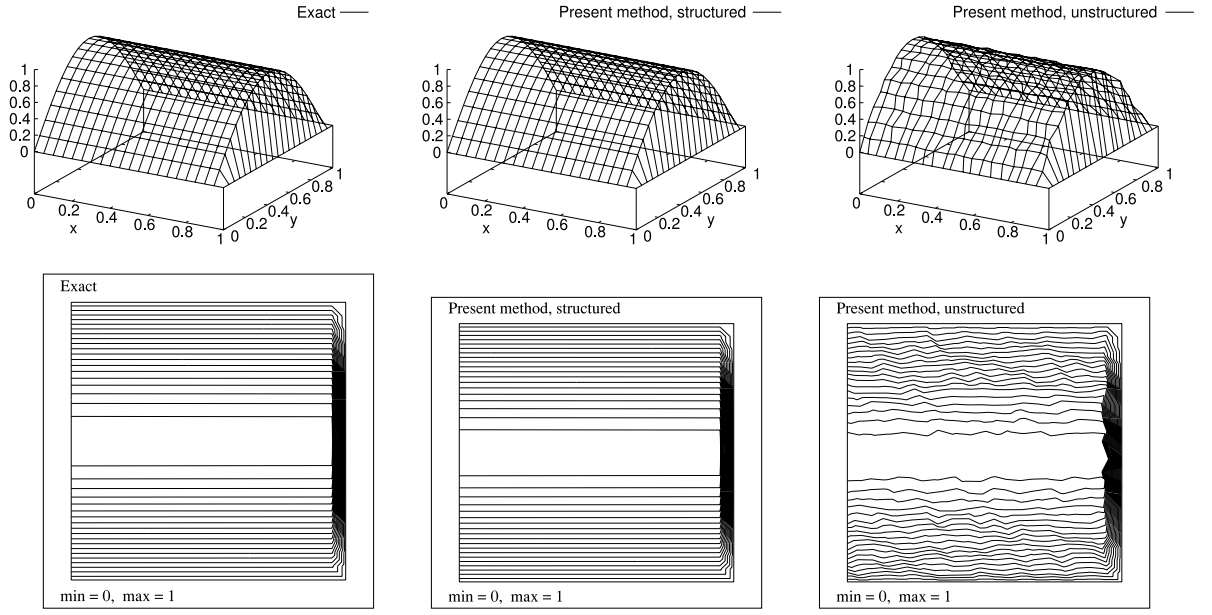

Fig. 5. Test 1, elevation plots and corresponding contour plots obtained with 21×21 nodes for $\sigma = 10^{-6}$ which corresponds $Pe = 500$.

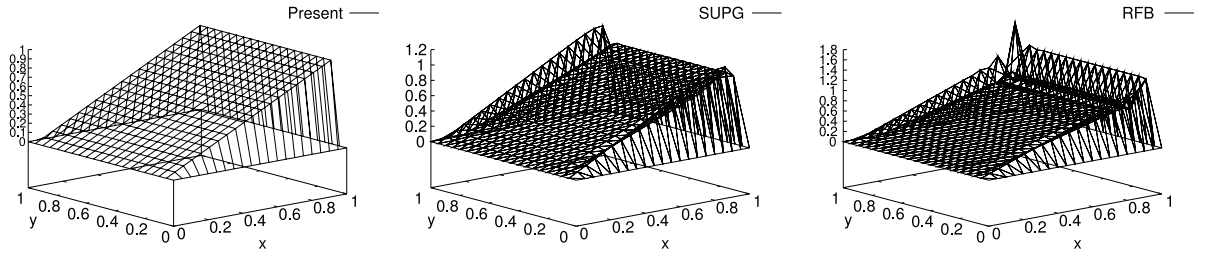

Fig. 6. Test 2, numerical solutions obtained with 21×21 nodes for $Pe = 50{,}000$.

$\sigma = 10^{-6}$, 15 with $\epsilon = 10^{-4}$. Quality of the present algorithm is clear for both cases. Fig. 5 presents elevation plots of exact solution and numerical approximations obtained with present method and corresponding contour plots for $\sigma = 10^{-6}$.

4.2. Test 2

This test is a uniform advection problem on unit square with a constant source term studied in [19]. The problem data is: $\epsilon = 10^{-6}$, $(b_1, b_2) = (1, 0)$, $\sigma = 0$ and $f = 1$ which corresponds to $Pe = 50{,}000$. Homogeneous Dirichlet boundary condition is imposed everywhere. Exact solution of this problem exhibits exponential layers at the boundary $(x = 1, y)$ and characteristic boundary layers at $(x, y = 0)$ and $(x, y = 1)$. Numerical solutions obtained with 21×21 uniform nodes, are presented in Fig. 6 and corresponding contour plots in Fig. 7. Although SUPG and RFB methods exhibit undesired oscillations near layers regions, Present method has no undesired oscillations.

4.3. Test 3

In this test, we observe behavior of the method in different regimes on unit square and compare with other methods. Homogeneous Dirichlet boundary condition is imposed everywhere on the boundary. We take $\epsilon = 10^{-6}$, $(b_1, b_2) = (\cos 72°, \sin 72°)$ and different intensities of reactions $\sigma = 10^{-6}, 20, 1000$ with $f = 1, 20, 1000$, respectively. Numerical solutions obtained with 21×21 uniform nodes are shown in Fig. 8.

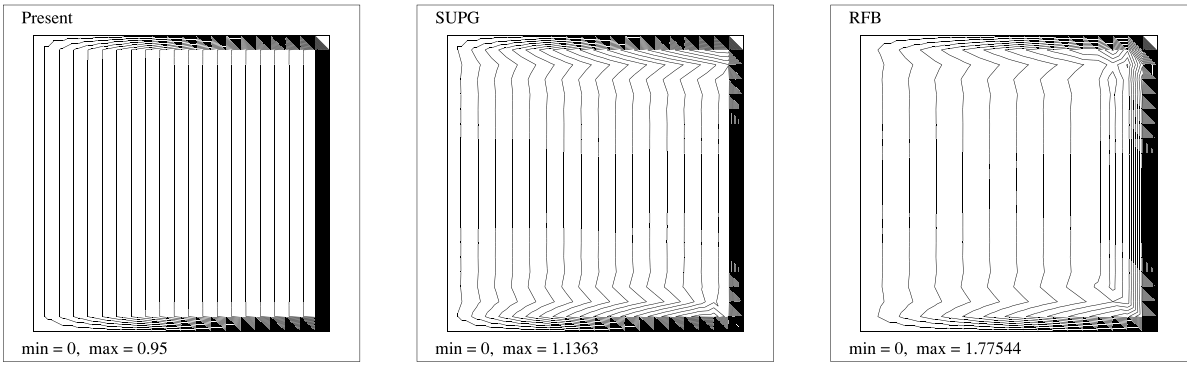

Fig. 7. Test 2, corresponding contour plots of numerical solutions in Fig. 6.

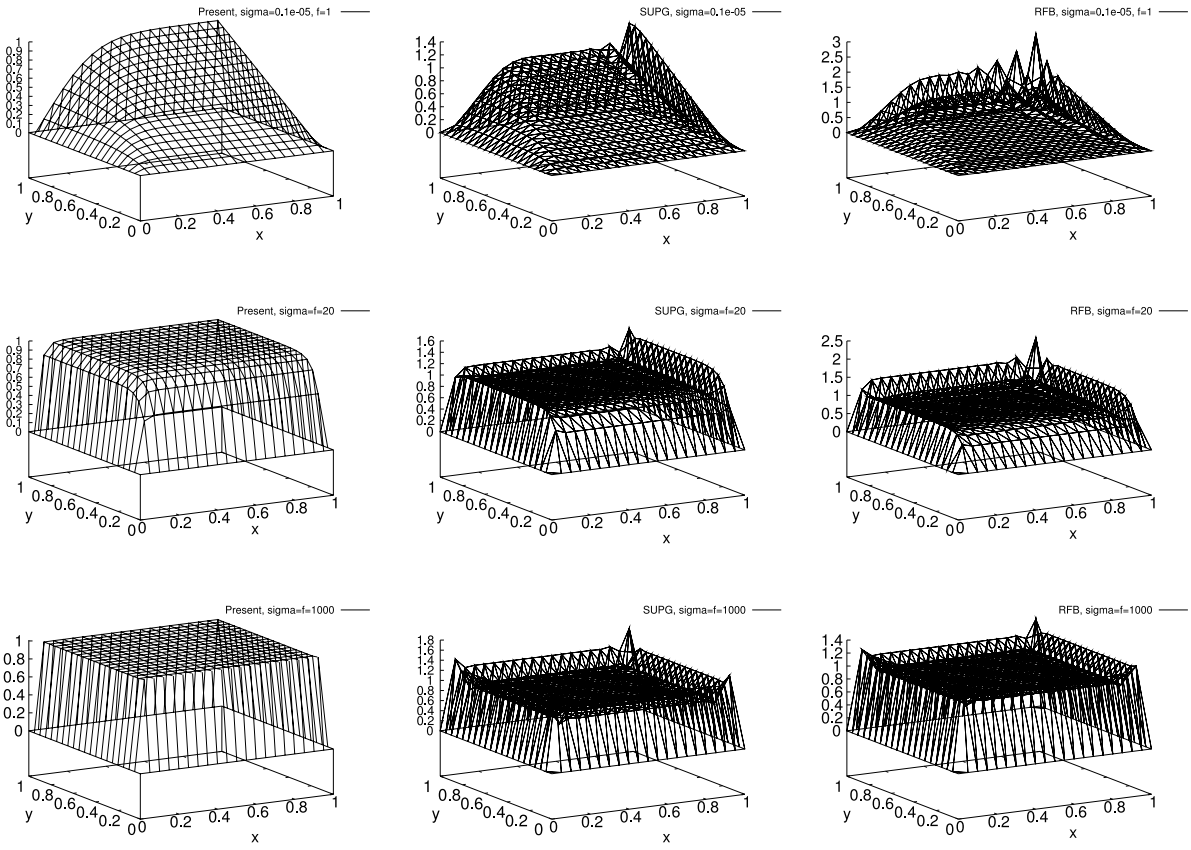

Fig. 8. Test 3, numerical solutions in different regimes for mesh Peclet and Damköhler numbers, $Pe = 50{,}000$, $Da = 0.00000005$ (first row), $Pe = 50{,}000$, $Da = 1$ (second row), $Pe = 50{,}000$, $Da = 50$ (third row).

4.4. Test 4

In this test problem we take the following boundary conditions which lead sharp boundary layers in reaction dominated regime:

$$u = \begin{cases} 0, & \text{if } y = 0,\ 0 \le x \le 1, \\ 0, & \text{if } x = 1,\ 0 \le y \le 1, \\ 1, & \text{if } y = 1,\ 0 \le x \le 1, \\ 1, & \text{if } x = 0,\ 0 \le y \le 1. \end{cases}$$

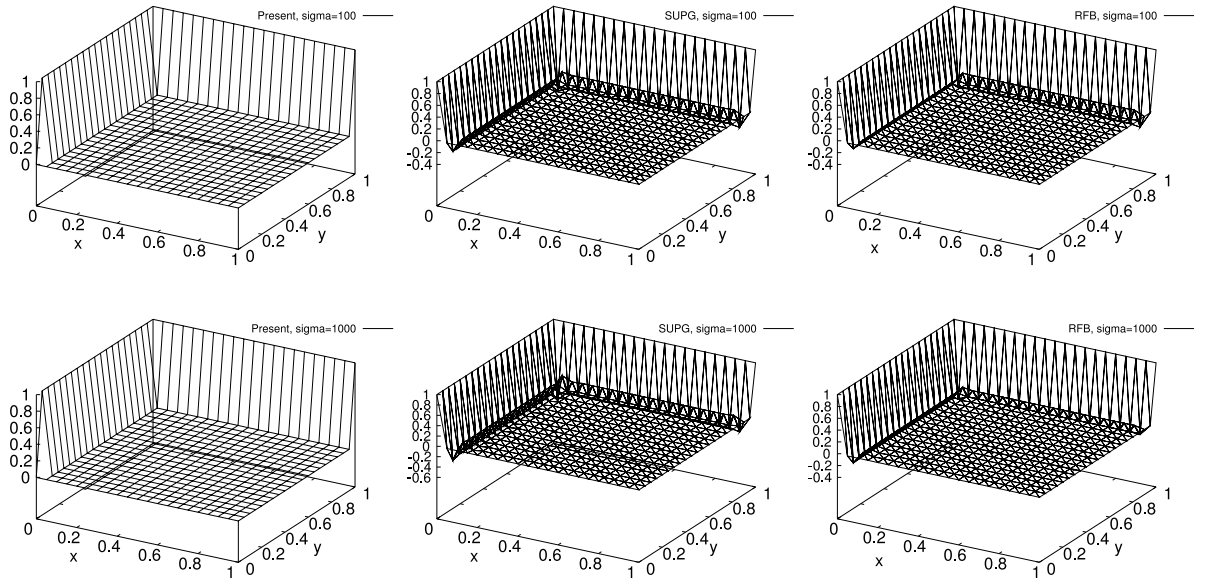

Fig. 9. Test 4, numerical approximations of the three methods for $Pe = 50{,}000$, $Da = 5$ (first row), $Pe = 50{,}000$, $Da = 50$ (second row).

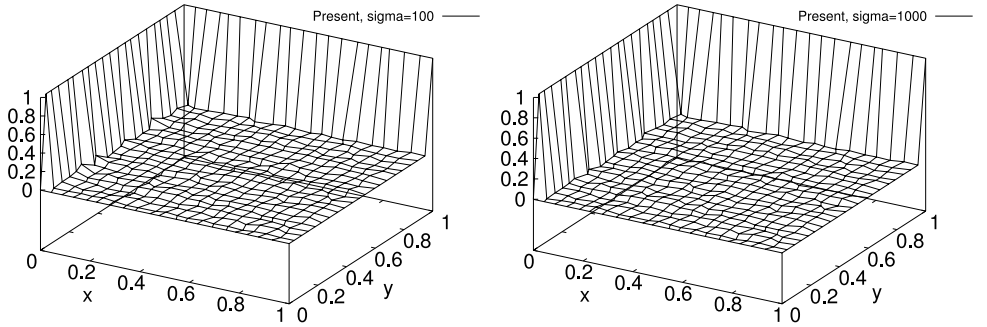

Fig. 10. Test 4, numerical approximations of the present method on unstructured grid.

We set diffusion coefficient to $\epsilon = 10^{-6}$ and angle of wind to $(b_1, b_2) = (\cos 45°, \sin 45°)$ with $f = 0$. Numerical solutions obtained with 21×21 structured grid are shown in Fig. 9 for $\sigma = 100, 1000$. Furthermore, numerical approximations for the same problem parameters obtained with 21×21 unstructured grid are presented in Fig. 10.

4.5. Test 5

In this test problem we consider the following boundary conditions on unit square which leads internal layer in the direction of the angle of wind when the problem is convection dominated:

$$u = \begin{cases} 1, & \text{if } y = 0, 0 \le x \le 0.2, \\ 0, & \text{if } y = 0, 0.2 < x \le 1, \\ 0, & \text{if } x = 1, 0 \le y \le 1, \\ 0, & \text{if } y = 1, 0 \le x \le 1, \\ 1, & \text{if } x = 0, 0 \le y \le 1. \end{cases}$$

The problem data is: $\epsilon = 10^{-6}$, $(b_1, b_2) = (\cos 75°, \sin 75°)$ $\sigma = 10^{-6}$ with $f = 0$. Fig. 11 shows elevation plots and corresponding contour plots of numerical approximations obtained with 41×41 uniform nodes. Moreover, numerical solution and corresponding contour plot of the present method for the same problem parameters obtained with unstructured grid points are illustrated in Fig. 12.

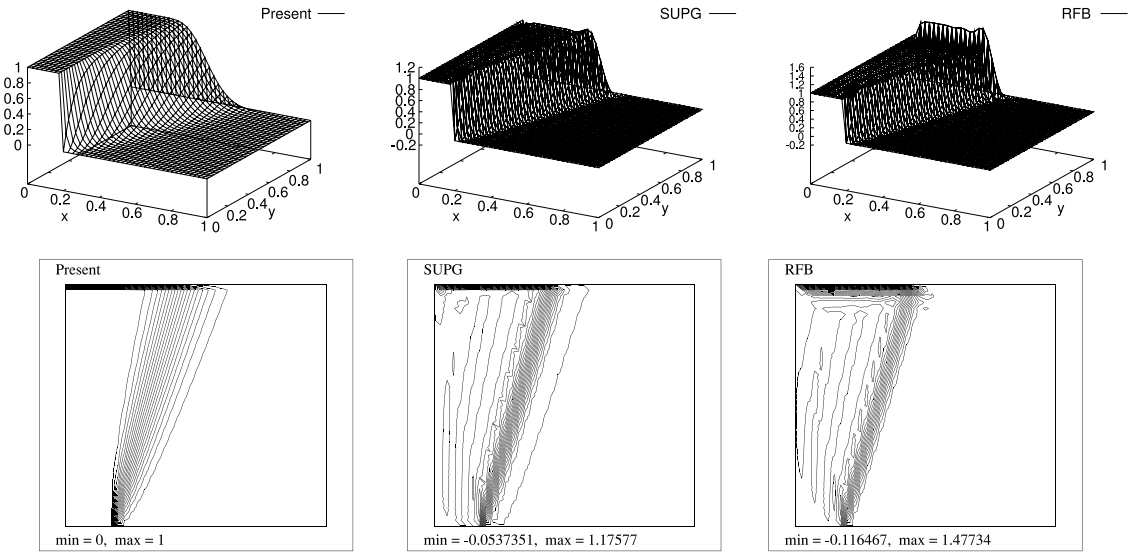

Fig. 11. Test 5, numerical solutions and corresponding contour plots of three methods for $Pe = 25{,}000$.

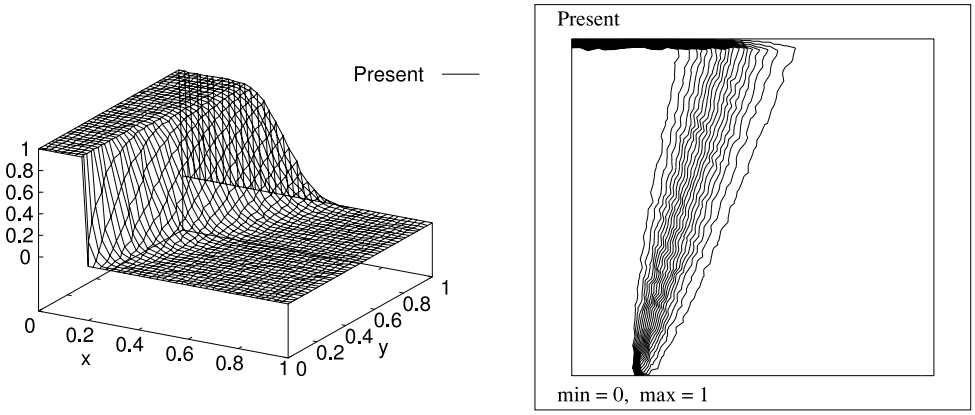

Fig. 12. Test 5, numerical solution of the present method on unstructured grid.

4.6. Test 6

Next, we consider a nonuniform advection problem. The boundary conditions are given by

$$u = \begin{cases} 1, & \text{if } x = 0, 0 \le y \le 1, \\ 0, & \text{otherwise.} \end{cases}$$

We set $\epsilon = 10^{-6}$, $(b_1, b_2) = (y, -x)$, $\sigma = 10^{-6}$, $f = 0$ and display the numerical results in Fig. 13 on 81×81 structured and unstructured grid points.

4.7. Test 7

This is a nonuniform advection and reaction problem. Consider the unit square and the following problem data: $\epsilon = 10^{-6}$, $(b_1, b_2) = (10x, 10y)$, $\sigma = x$ and $f = 0$. The Dirichlet boundary conditions are: $u = 1$ on $(x = 0, y)$ and $u = 0$ on the rest of the boundary. The domain is discretized using 41×41 structured and unstructured grid points. Numerical solutions are presented in Fig. 14.

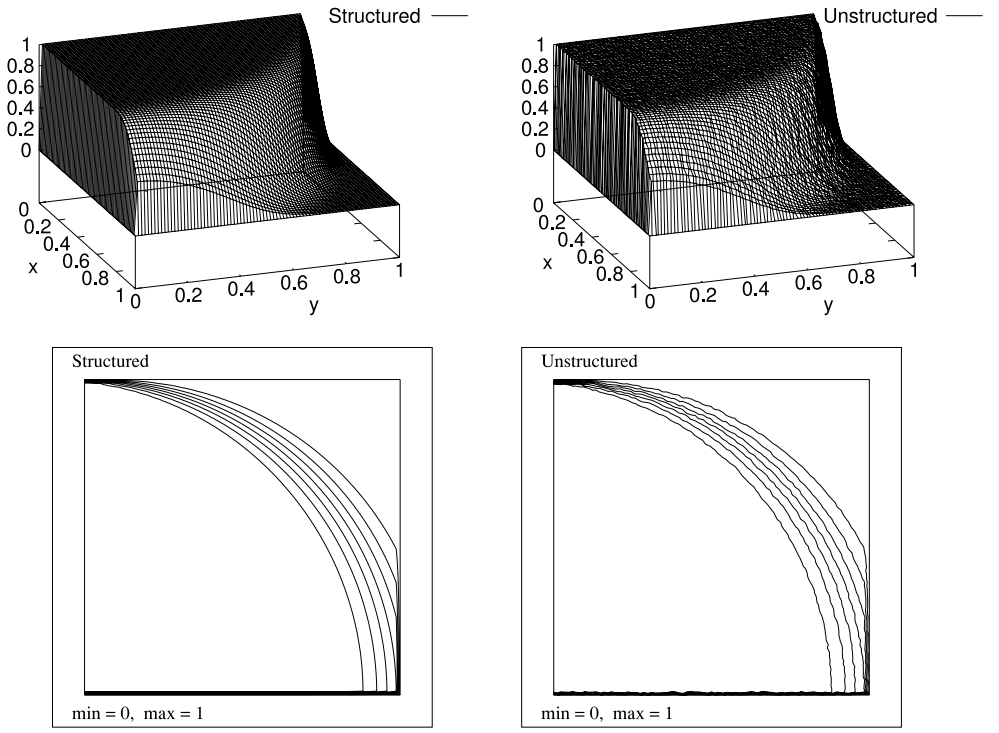

Fig. 13. Test 6, elevation plots and corresponding contour plots of the present method for nonuniform advection.

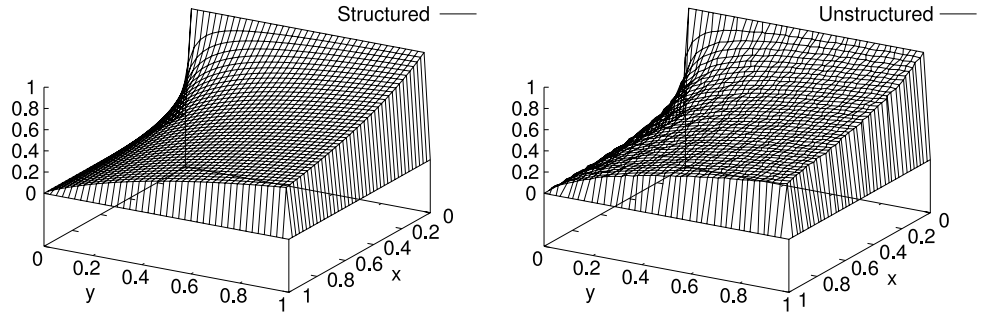

Fig. 14. Test 7, numerical approximations on structured and unstructured grids.

4.8. Test 8

In this test problem, we consider a half circular domain centered at the point $(0.5, 0)$ with radius $r = 0.5$. 961 structured (nonuniform) grid points are used for the discretization of the domain. The Dirichlet boundary conditions are: $u = 1$ on $(0 \leq x \leq 0.5, y = 0)$ and $u = 0$ on the rest of the boundary. The problem data is $\epsilon = 10^{-6}$, $\sigma = 10^{-6}$, $(b_1, b_2) = (0, 1)$ and $f = 0$. The grid used in numerical approximation and elevation plot of numerical solution are illustrated in Fig. 15.

4.9. Test 9

This is a convection–diffusion problem with variable source function. Homogeneous Dirichlet boundary condition is imposed everywhere on the boundary on unit square. The problem data is $\epsilon = 10^{-7}$, $\sigma = 0$, $(b_1, b_2) = (\cos 72^\circ, \sin 72^\circ)$ and $f = x + y$. Numerical solutions obtained with 41×41 structured and unstructured grid points are presented in Fig. 16.

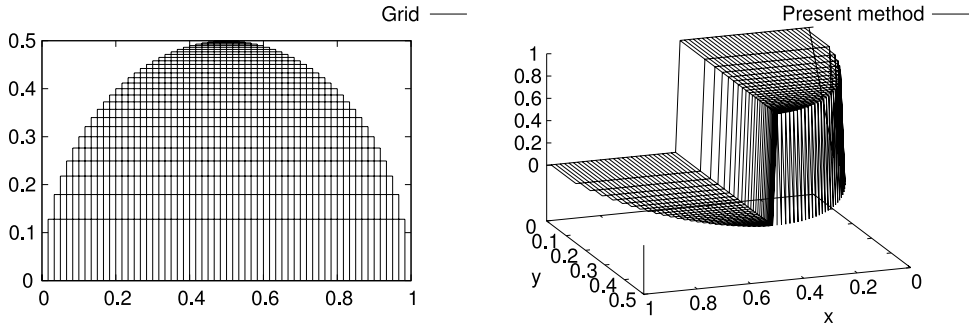

Fig. 15. Test 8, the grid used in numerical approximation and elevation plot of numerical solution.

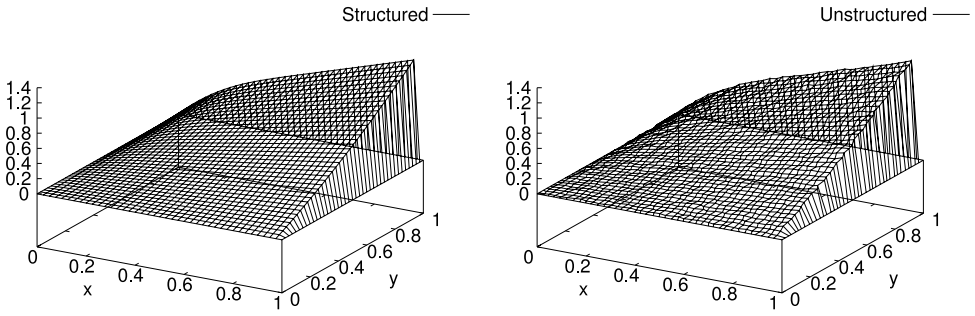

Fig. 16. Test 8, numerical solutions on structured and unstructured grids for $Pe = 125{,}000$.

4.10. Test 10

This is the last test problem in two space dimensions. We consider a variable source function which is discontinuous and defined as follows:

$$f(x, y) = \begin{cases} 200x, & \text{if } 0 \le x \le 0.5, \\ -200x, & \text{if } 0.5 < x \le 1. \end{cases}$$

Homogeneous Dirichlet boundary condition is imposed everywhere on the boundary. We take $\epsilon = 10^{-6}$, $\sigma = 200$ and $(b_1, b_2) = (0, 1)$. Numerical approximations obtained with 21×21 and 41×41 uniform grid points are presented in Fig. 17.

4.11. Test 11

In our last experiment, we apply the method to 3-dimensional convection–diffusion–reaction equation. We test the method for different intensities of reactions. Homogeneous Dirichlet boundary condition is imposed everywhere on unit cube. $21 \times 21 \times 21$ uniform grid points are used to discretize the domain. We take $\epsilon = 10^{-6}$, $(b_1, b_2, b_3) = (0, 0, 1)$ and different intensities of reactions $\sigma = 10^{-6}, 10, 50, 1000$ with $f(x, y, z) = 1, 10, 50, 1000$ on $0.2 \le x \le 0.5$, $0.2 \le y \le 0.5$, $0.2 \le z \le 0.5$ and it is zero elsewhere in the domain. Numerical solutions at the cut plane $x = 0.5$ are presented in Fig. 18.

5. Conclusion

In this paper, a finite difference method was proposed for multidimensional convection–diffusion–reaction equations. This approach is highly based on the work [15] which was proposed for one dimensional convection–diffusion–reaction equation. Derivation of the algorithm in two and three space dimensions is based on a simplistic split to two and three expressions, respectively and then joining together their approximations. Stencils for uniform and nonuniform grid points were derived. In the numerical studies, we tested the present algorithm in different regimes

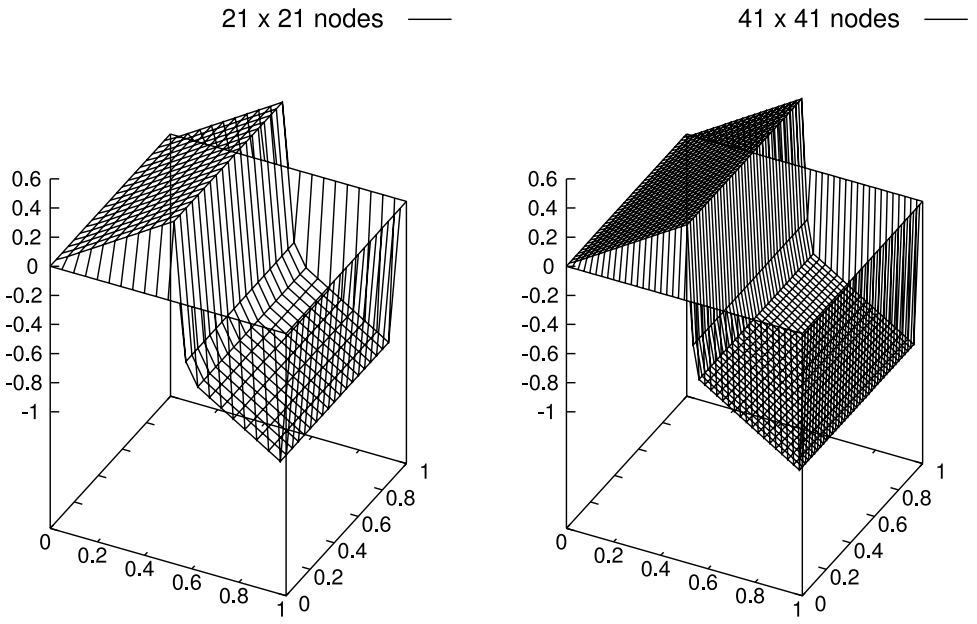

Fig. 17. Test 9, numerical approximations of test problem 6 for $Da = 10$ (left) and $Da = 5$ (right).

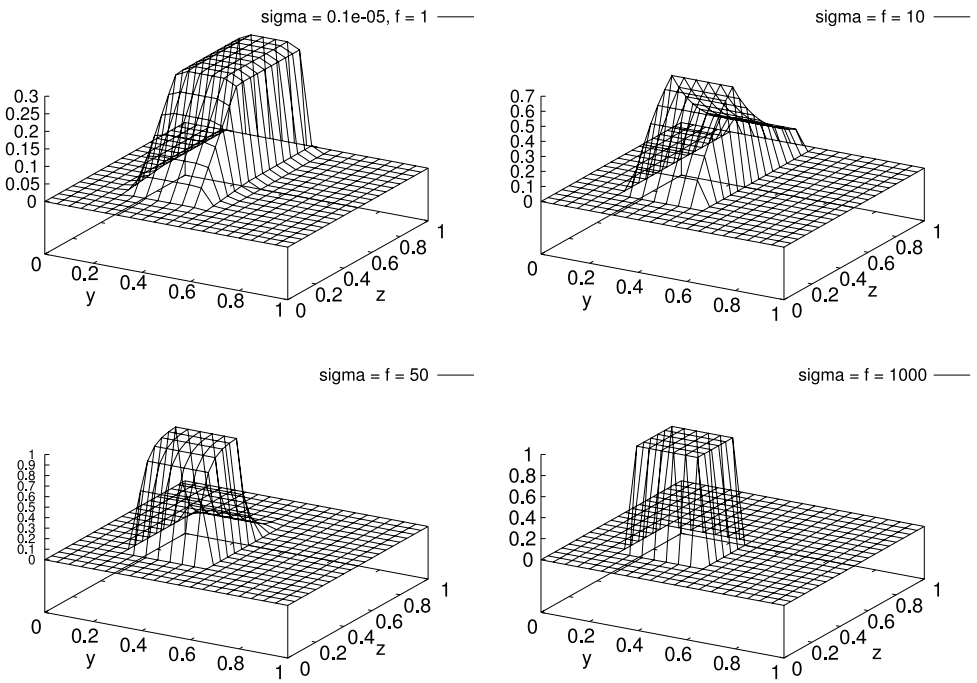

Fig. 18. Test 10, numerical approximations at the cut plane $x = 0.5$. The mesh Peclet number is $Pe = 25{,}000$ and Damköhler numbers are $Da = 0.00000005$ for $\sigma = 10^{-6}$, $Da = 0.5$ for $\sigma = 10$, $Da = 2.5$ and $Da = 50$ for $\sigma = 1000$.

and compared it with well known stabilized finite element methods. Comprehensive comparisons indicated superiority of the present method. Since the pseudo basis bubble functions in [15] effectively approximate the basis bubble functions in one space dimension and it is very difficult to approximate the bubbles in higher dimensions efficiently, the present method leads to superior numerical performance than RFB method. The method was tested for wide ranges of the problem coefficients. We increased the mesh Peclet number (Pe) up to 125,000 and Damköhler number (Da) up

to 50 and we encountered ignorable oscillations on unstructured grids just for some tests. Furthermore, a half circular domain which was discretized by nonuniform grid points was used to show that the present method is applicable in complex domains. Finally, we applied the method to 3-dimensional convection–diffusion–reaction problem and we saw that the quality is preserved in three space dimensions.

References

[1] A.N. Brooks, T.J.R. Hughes, Streamline upwind/Petrov–Galerkin formulations for convection dominated flows with particular emphasis on the incompressible Navier–Stokes equations, Comput. Methods Appl. Mech. Engrg. 32 (1982) 199–259.
[2] M.I. Asensio, A. Russo, G. Sangalli, The Residual-Free Bubble numerical method with quadratic elements, Math. Models Methods Appl. Sci. 14 (2004) 641–661.
[3] C. Baiocchi, F. Brezzi, L.P. Franca, Virtual bubbles and the GaLS, Comput. Methods Appl. Mech. Engrg. 105 (1993) 125–141.
[4] F. Brezzi, A. Russo, Choosing bubbles of advection–diffision problems, Math. Models Methods Appl. Sci. 4 (1993) 571–587.
[5] F. Brezzi, M.O. Bristeau, L.P. Franca, M. Mallet, G. Roge, A relationship between stabilized finite element methods and the Galerkin method with bubble functions, Comput. Methods Appl. Mech. Engrg. 96 (1992) 117–129.
[6] F. Brezzi, G. Hauke, L.D. Marini, G. Sangalli, Link-cutting bubbles for the stabilization of convection–diffusion–reaction problems, Math. Models Methods Appl. Sci. 13 (2003) 445–461.
[7] F. Brezzi, L.D. Marini, A. Russo, Applications of pseudo residual-free bubbles to the stabilization of convection–diffusion problems, Comput. Methods Appl. Mech. Engrg. 166 (1998) 51–63.
[8] F. Brezzi, L.D. Marini, A. Russo, On the choice of a stabilizing subgrid for convection–diffusion problems, Comput. Methods Appl. Mech. Engrg. 194 (2004) 127–148.
[9] F. Brezzi, L.D. Marini, Augmented spaces, two-level methods, and stabilizing subgrids, Internat. J. Numer. Methods Fluids 40 (2002) 31–46.
[10] L.P. Franca, F.-N. Hwang, Refning the submesh strategy in the two-level finite element method: application to the advection-diffusion equation, Internat. J. Numer. Methods Fluids 39 (1998) 161–187.
[11] L.P. Franca, A.I. Neslitürk, M. Stynes, On the stability of residual-free bubbles for convection–diffusion problems and their approximation by a two-level finite element method, Comput. Methods Appl. Mech. Engrg. 166 (1998) 35–49.
[12] A.I. Neslitürk, On the choice of stabilizing sub-grid for convection–diffusion problem on rectangular grids, Comput. Math. Appl. 59 (2010) 3687–3699.
[13] A.I. Neslitürk, S.H. Aydin, M.T. Sezgin, Two-level finite element method with a stabilizing subgrid for the incompressible Navier–Stokes equations, Internat. J. Numer. Methods Fluids 58 (2008) 551–572.
[14] A. Sendur, A. Neslitürk, A. Kaya, Applications of the pseudo residual-free bubbles to the stabilization of the convection–diffusion–reaction problems in 2D, Comput. Methods Appl. Mech. Engrg. 277 (2014) 154–179.
[15] A. Şendur, A.I. Neslitürk, Applications of the pseudo residual-free bubbles to the stabilization of convection–diffusion–reaction problems, Calcolo 49 (2011) 1–19.
[16] G. Hauke, M.H. Doweidar, Fourier analysis of semi-discrete and space–time stabilized methods for the advective–diffusive–reactive equation: I. SUPG, Comput. Methods Appl. Mech. Engrg. 194 (2005) 45–81.
[17] G. Hauke, M.H. Doweidar, Fourier analysis of semi-discrete and space–time stabilized methods for the advective–diffusive–reactive equation: II. SGS, Comput. Methods Appl. Mech. Engrg. 194 (2005) 45–81.
[18] G. Hauke, M.H. Doweidar, Fourier analysis of semi-discrete and space–time stabilized methods for the advective–diffusive–reactive equation: III. SGS/GSGS, Comput. Methods Appl. Mech. Engrg. 195 (2005) 691–725.
[19] P. Nadukandi, E. Oate, J. Garca, A high-resolution Petrov–Galerkin method for the convection–diffusion–reaction problem. Part II-A multidimensional extension, Comput. Methods Appl. Mech. Engrg. 213–216 (2012) 327–352.